

## Modelling and Optimization of an Electrohydrodynamic (EHD) Thruster

Victor H. Granados<sup>1</sup>, Mario J. Pinheiro<sup>2</sup> and Paulo A. Sá<sup>1</sup>

<sup>1</sup> *Departamento de Engenharia Física, Faculdade de Engenharia da Universidade do Porto  
Rua Doutor Roberto Frias s/n 4200-465, Porto, Portugal*

<sup>2</sup> *Departamento de Física, Instituto Superior Técnico - IST  
Universidade de Lisboa, Av. Rovisco Pais, 1049-001 Lisboa, Portugal*

### Abstract

*A theoretical self-consistent two dimensional model of an axisymmetric electrostatic plasma actuator is presented. The computational model solves the governing equations for a plasma kinetic model using the software COMSOL MULTIPHYSICS for discharges using three different gases independently: argon, nitrogen and oxygen at a pressure of 0.5 Torr. In the argon scenario, we include the following heavy (neutral and charged) species: Ar(X), Ar\* and Ar<sup>+</sup> while the nitrogen scenario includes: N, N<sup>+</sup>, N<sub>2</sub>, N<sub>2</sub><sup>+</sup> and N<sub>4</sub><sup>+</sup> and the oxygen scenario considers: O, O<sup>+</sup>, O<sup>-</sup>, O<sub>2</sub>, O<sub>2</sub><sup>+</sup> and O<sub>2</sub><sup>-</sup>.*

### Introduction

Since the discovery of the ionic wind effect in 1709 by Francis Hauksbee [1] there is a rising interest in EHD thrusters as a useful mean to convert electric energy into kinetic energy. The mechanism of a EHD thruster consists in an applied electric field that accelerates the electrically charged particles while collisional coupling ensures the momentum transfer between ions and neutrals [2]. The electrically neutral particles are ionized in the region surrounding the electrode with smaller curvature radius (anode on the present case) due to the higher electric field on its surface, which is the well-known Corona Effect [3]. The charged particles flow towards the electrodes, depending on their charge, where they are collected. For the discharge to be sustained, a secondary electron emission must occur at the cathode, that is due to the impact of ions on its surface and its effect is essential for the stability of the mechanism.

### Thruster model

The model consists of a set of differential equations modelling the different phenomena taking place in a DC-discharge. The electrostatic field is computed using the Poisson equation ( $\epsilon \nabla^2 V = -\rho$ , where  $\epsilon$  is the plasma permittivity ( $\epsilon = \epsilon_0 \epsilon_r$ ),  $V$  is the electric potential and  $\rho$  is the space charge density), which is computed through the plasma chemistry by the equation:

$$\rho = e \left( \sum_{j=1}^N Z_j n_j - n_e \right) \quad (1)$$

where  $Z_j$  is the charge number of ions,  $n_j$  and  $n_e$  are the ions and electron densities, respectively. For the electron-impact reactions considered on the model, we assumed a Maxwellian distribution function and computed the rate coefficients from the equation:

$$k_j = \left(\frac{2e}{m_e}\right)^{1/2} \int_0^\infty u \sigma_j(u) f(u) du \quad (2)$$

where  $u$  is the electron energy (eV) and  $\sigma_j(u)$  represents the elastic and inelastic (excitation and ionization) cross sections considered for each reaction.

The fluid is assumed to be quasi-steady, with a small Mach number ( $M < 0.3$ ), and although it is often account as incompressible, for simulation purposes we considered the compressible fluid Navier-Stokes equations described by the following equation, which includes variations in the space charge density as depicted by the continuity equation:

$$\begin{aligned} \rho \frac{\partial \mathbf{u}}{\partial t} + \rho (\mathbf{u} \cdot \nabla) \mathbf{u} &= -\nabla p + \nabla \cdot \left[ \mu (\nabla \mathbf{u} + (\nabla \mathbf{u})^T) - \frac{2}{3} \mu (\nabla \cdot \mathbf{u}) \mathbf{I} \right] + \mathbf{F} \\ \frac{\partial \rho}{\partial t} + \nabla \cdot (\rho \mathbf{u}) &= 0 \end{aligned} \quad (3)$$

where  $\mathbf{u}$  is the fluid velocity,  $p$  is the pressure,  $\mu$  is the dynamic viscosity,  $\mathbf{I}$  is the identity matrix and  $\mathbf{F}$  is the volume force vector, which comes from the integration of the force density ( $\mathbf{f} = \rho \mathbf{E}$ ) all over the volume. A RC coupling circuit is used in series with the DC source in order to avoid the arc regime between its electrodes.

Table 1: Rate coefficients

(a) Argon discharge			(b) Nitrogen discharge			(c) Oxygen discharge		
Reaction	Rate coefficient [ $m^3/s$ or $m^6/s$ ]	Ref.	Reaction	Rate coefficient [ $m^3/s$ or $m^6/s$ ]	Ref.	Reaction	Rate coefficient [ $m^3/s$ or $m^6/s$ ]	Ref.
$e + Ar \rightarrow e + Ar$	$\sigma(u)$	[4]	$e + N_2 \rightarrow e + N_2$	$\sigma(u)$	[7]	$e + O \rightarrow e + O$	$\sigma(u)$	[4]
$e + Ar \rightarrow e + Ar^*$	$\sigma(u)$	[4]	$e + N_2 \rightarrow 2e + N_2^+$	$\sigma(u)$	[7]	$e + O_2 \rightarrow e + O_2$	$\sigma(u)$	[4]
$e + Ar \rightarrow 2e + Ar^+$	$\sigma(u)$	[4]	$e + N_2 \rightarrow e + 2N$	$\sigma(u)$	[8]	$e + O_2 \rightarrow e + 2O$	$\sigma(u)$	[4]
$e + Ar^* \rightarrow 2e + Ar^+$	$\sigma(u)$	[4]	$e + N_2^+ \rightarrow 2N$	$2.8 \times 10^{-13} (300/T_e)^{0.5}$	[9]	$e + O_2 \rightarrow 2e + O_2^+$	$\sigma(u)$	[4]
$Ar^* + Ar^* \rightarrow e + Ar + Ar^+$	$6.2 \times 10^{-16}$	[5], [6]	$e + N_2^+ + N_2 \rightarrow 2N_2$	$2.6 \times 10^{-39} (300/T_e)^{1.5}$	[9]	$e + O_2 \rightarrow O_2^-$	$\sigma(u)$	[4]
$Ar^* + Ar \rightarrow Ar + Ar$	$3.0 \times 10^{-21}$	[5], [6]	$e + N_2^+ \rightarrow N_2$	$1 \times 10^{-25} (T_g/T_e)^{4.5}$	[9]	$2e + O_2^+ \rightarrow e + O_2$	$1 \times 10^{-31} (300/T_e)^{4.5}$	[9]
			$e + N_4^+ \rightarrow N_2 + N_2$	$2 \times 10^{-12} (T_g/T_e)^{0.5}$	[9]	$e + O_2^+ + O_2 \rightarrow 2O_2$	$6 \times 10^{-39} (300/T_e)^{1.5}$	[9]
			$N_2^+ + N \rightarrow N^+ + N_2$	$7.2 \times 10^{-19} \exp(T_g/300)$	[9]	$e + O_2^+ \rightarrow O + O$	$2 \times 10^{-13} (300/T_e)$	[9]
			$N_4^+ + N_2 \rightarrow N_2^+ + 2N_2$	$2.1 \times 10^{-22} \exp(T_g/121)$	[9]	$e + O + O_2 \rightarrow O + O_2^-$	$1 \times 10^{-43}$	[9]
			$N_2^+ + 2N_2 \rightarrow N_4^+ + N_2$	$5.0 \times 10^{-41}$	[9]	$e + O + O_2 \rightarrow O^- + O_2$	$1 \times 10^{-43}$	[9]
						$O^+ + O + O_2 \rightarrow O_2^+ + O_2$	$1 \times 10^{-41}$	[9]
						$O^+ + O_2 \rightarrow O_2^+ + O$	$3.3 \times 10^{-17} \exp(-0.00169T_g)$	[9]
						$O_2^- + O \rightarrow O^- + O_2$	$3.3 \times 10^{-16}$	[10]
						$O^- + O \rightarrow O_2 + e$	$1.4 \times 10^{-16}$	[10]
						$O_2^- + O_2 \rightarrow 2O_2 + e$	$2.7 \times 10^{-16} (T_g/300)^{0.5} \exp(-5590/T_g)$	[10]

We considered self-consistent kinetic models for each gas, which includes electron-impact reactions (elastic, excitation and ionization), and chemical reactions in order to model the

behaviour of the gas during the discharge. The reaction rates of the kinetic models are detailed in Table 1. The simulation conditions were:  $P = 0.5 \text{ Torr}$ ,  $T_g = 300 \text{ K}$ ,  $V = 250 \text{ V}$ ,  $R = [20 - 1500] \text{ k}\Omega$  and  $C = 1 \text{ pF}$ .

## Results and discussions

Figure 1 shows the electron density distributions for the three gases considered. Nitrogen showed at least two orders of magnitude greater than oxygen and than argon.

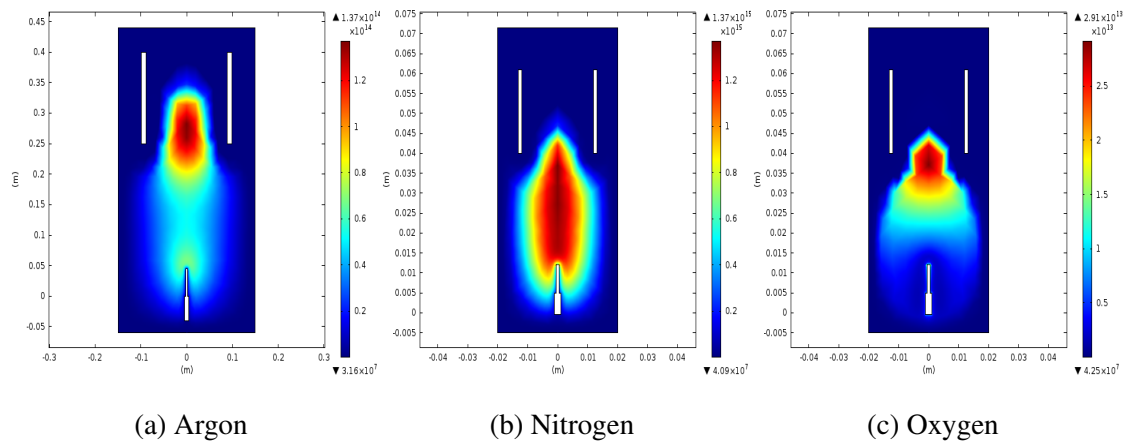


Figure 1: Electron density distributions ( $m^{-3}$ )

Figure 2 shows the fluid speed distributions for the three gases. In argon, the speed is two orders of magnitude less than in nitrogen and the configuration shows a very different profile which is due to a less inefficient momentum transfer. Nitrogen gas presents the highest peak speed ( $12.5 \text{ cm/s}$ ) which indicates a more efficient ionic wind phenomenon.

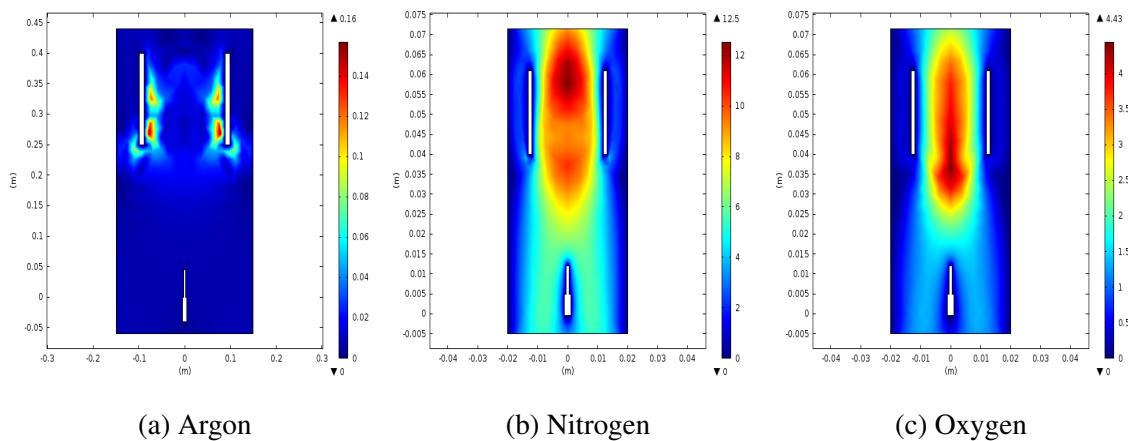


Figure 2: Fluid velocity distributions ( $cm/s$ )

In order to calculate the total thrust produced by the flux of gas going through the EHD thruster, we integrate over the output of the thruster. Table 2 shows the net thrust produced using the different gasses in the thruster's chamber, along with the power consumption and the

Thrust-to-Power (F/P) ratio, a known parameter to determine the amount of thrust obtained for a given power input. According to Masuyama et al. [3]: “EHD thrusters have documented thrust-to-power ratios as high as  $26 \text{ mN/W}$ , which is orders of magnitude greater than electrostatic propulsion systems used in space”

Table 2: Net thrust produced by EHD thruster using different gases

Gas	Thrust ( $nN$ )	Power ( $mW$ )	Thrust-to-Power ratio ( $nN/W$ )
$Ar$	$9.77 \times 10^{-4}$	38.1	$2.56 \times 10^{-2}$
$N_2$	3.86	183.1	21.1
$O_2$	0.331	10.4	31.8

Nitrogen gas presents the highest thrust production among the gases considered (ten times higher than oxygen), however, oxygen presented a higher Thrust-to-Power ratio which indicates a higher efficiency in transforming electric energy into thrust. Argon gas produced the fewest amount of thrust, as well as the lowest Thrust-to-Power ratio.

### Conclusions and future work

We conclude that argon contributes with the smallest thrust due to its mono-atomicity nature while nitrogen produces the highest thrust due to the  $N_2^+$  ions, the most effective conveyors of momentum to the neutrals. The oxygen was more efficient in transforming power to thrust but generated a total net thrust four times smaller than nitrogen's. We corroborated that plasma actuators produce thrust in presence of different gases ( $Ar$ ,  $N_2$  and  $O_2$ ) with high energy-conversion performance and thus consists in a attractive technology for near future aerospace applications. Although our thruster is far from a commercial application, we proved the feasibility of simulating the ionic wind phenomena which will lead us to an optimization process until we reach a better EHD thruster.

### References

- [1] Hauksbee, F., Physico-Mechanical Experiments on Various Subjects, London, (1709), 1st Edition, pp. 46-47.
- [2] Alexandre A. Martins and Mario J. Pinheiro, Phys. Plasmas **18**, 033512 (2011) <http://dx.doi.org/10.1063/1.3562874>.
- [3] Masuyama, K. and Barrett, S. R. H., On the performance of electrohydrodynamic propulsion. Proc. R Soc. A, (2013), **469**: 20120623.
- [4] Morgan database, www.lxcat.net, retrieved on January 25, (2015).
- [5] Bogaerts, A. and Gijbels, R., Modeling of metastable argon atoms in a direct-current glow discharge, Physical Review A. **52** (1995).
- [6] Lam, S. K., Zheng, C-E, Lo, D., Dem'yanov, A. and Napartovich, A. P., Kinetics of  $Ar_2^*$  in high-pressure pure argon, Journal of Physics D: Applied Physics **33**, (2000) 242.
- [7] IST-Lisbon database, www.lxcat.net, retrieved on January 25, (2015).
- [8] Itikawa database, www.lxcat.net, retrieved on January 25, (2015).
- [9] Kossyi, I.A., Kostinsky, A.Y., Matveyev, A.A. and Silakov, V.P. Plasma Sources Sci. Technol. **1** (1992) 207.
- [10] Tatarova, E., Dias, F. M., Ferreira, C. M., Guerra, V., Loureiro, J., Stoykova, E., Ghanashev, I. and Zhelyazkov, I., Self-consistent kinetic model of a surface-wave-sustained discharge in nitrogen. J. Appl. Phys. (1997), **30**, 2663-2676.